17 (2023) 100262

Contents lists available at ScienceDirect

International Journal of Thermofluids

journal homepage: www.sciencedirect.com/journal/international-journal-of-thermofluids

Energy assessment of an integrated hydrogen production system

Mohamed S. Shahin [a], Mehmet F. Orhan [a,*], Kenan Saka [b], Ahmed T. Hamada [a], Faruk Uygul [c]

[a] Department of Mechanical Engineering, American University of Sharjah, United Arab Emirates
[b] Vocational School of Yenisehir Ibrahim Orhan, Bursa Uludag University, PO Box: 16900, Yenisehir, Bursa, Turkey
[c] Faculty of Science - Mathematics & Statistical Sciences, University of Alberta, Canada

ARTICLE INFO

Keywords:
Hydrogen production
Solar
Rankine cycle
Thermodynamic analysis
Electrolyzer
Parabolic trough
Heliostat field

ABSTRACT

Hydrogen is believed to be the future energy carrier that will reduce environmental pollution and solve the current energy crisis, especially when produced from a renewable energy source. Solar energy is a renewable source that has been commonly utilized in the production process of hydrogen for years because it is inexhaustible, clean, and free. Generally, hydrogen is produced by means of a water splitting process, mainly electrolysis, which requires energy input provided by harvesting solar energy. The proposed model integrates the solar harvesting system into a conventional Rankine cycle, producing electrical and thermal power used in domestic applications, and hydrogen by high temperature electrolysis (HTE) using a solid oxide steam electrolyzer (SOSE). The model is divided into three subsystems: the solar collector(s), the steam cycle, and an electrolysis subsystem, where the performance of each subsystem and their effect on the overall efficiency is evaluated thermodynamically using first and second laws. A parametric study investigating the hydrogen production rate upon varying system operating conditions (e.g. solar flux and area of solar collector) is conducted on both parabolic troughs and heliostat fields as potential solar energy harvesters. Results have shown that, heliostat-based systems were able to attain optimum performance with an overall thermal efficiency of 27% and a hydrogen production rate of 0.411 kg/s, whereas, parabolic trough-based systems attained an overall thermal efficiency of 25.35% and produced 0.332 kg/s of hydrogen.

1. Introduction

Energy plays a crucial role in human life. The enormous increase in the use of technological equipment, machinery, and devices requires energy now more than ever. Energy requirements are not only dependent on domestic use, but also on activities such as agriculture, construction, manufacturing, and other industries. With the rapid rise of technology over the past century, solutions are required to accelerate the production of energy. Population growth and the desire to raise the standard of living are what primarily drive the energy demand. Clean energy sources are now needed to protect the environment and make our lives more productive, safer, and healthier. Many countries have shown an active interest in renewable energy sources for meeting their energy demands without relying on fossil fuels. The burning of fossil fuels increases environmental pollution and climate change. The dependency on fossil fuels to be the future unique energy source raises doubts. The depletion of those fuels over time and the increase in prices of oil and gas require alternative energy sources. In the Arabian Gulf region, especially in the United Arab Emirates (UAE), the demand for energy is increasing and the most convenient renewable energy source available is solar energy. In the future, fossil fuels will no longer be the main energy source, with hydrogen being the energy carrier, making it appealing to utilize the solar energy available. Hydrogen is a very promising future energy carrier due to its many advantages. The use of solar energy in the UAE is slowly increasing due to the promising performance of the systems and the increase in research topics of systems utilizing solar energy. Recent research studies have been conducted on harvesting solar energy with existing systems such as the Rankine cycle with hydrogen production using water electrolysis.

Parabolic trough solar collectors are a type of concentrating collectors used in thermal power plants. They consist of a reflective mirror in the shape of a parabola, a tubular receiver, and support structures. The collector uses the solar incident rays from the sun, reflecting them onto a tubular receiver containing a heat transfer fluid (HTF) to produce heat. This heat is then used to convert water to superheated steam in a Rankine cycle to produce electricity. The tubular receiver sits at the focal point of the parabola for effective reflection of the sun's rays onto the fluid inside the receiver.

For centralized heat production using high temperature solar

* Corresponding author.
E-mail address: morhan@aus.edu (M.F. Orhan).

https://doi.org/10.1016/j.ijft.2022.100262

Available online 5 December 2022

Nomenclature

$\dot{m}$	Mass flow rate
Cp	Specific heat
T	Temperature
A	Area
F_R	Heat removal factor
S	Heat absorbed by receiver
U	Collector heat loss coefficient
D	Diameter
L	Length
G_b	Solar irradiation
w	Width
h	Heat transfer coefficient
Re	Reynolds number
V	Velocity
Col	Number of solar collectors
$\dot{Q}$	Heat rate
h	Enthalpy
F_r	View factor
C	Concentration ratio
d	Diameter
$\dot{W}$	Power output

Greek Letters

η	Efficiency
σ	Stefan Boltzmann constant
υ	Kinematic viscosity
ρ	Density
ε_w	Wall's emissivity
δ	Thickness
λ	Thermal conductivity

Subscripts

ri	Receiver's inlet
ro	Receiver's outlet
i	Inner
o	Outer
r	Receiver
ap	Aperture
c	Cover
a	Ambient
c,o	Cover outlet
c,i	Cover inlet
r,int	Internal receiver
0	Ambient
th	Thermal
rec	Receiver
s	Solar
rec,sur	Surface of receiver
insi	Inside
H	Heliostat field
em	Emissive heat
ref	Reflective heat
conv	Convective heat
cond	Conductive heat
H2	Hydrogen
insu	Insulation
ms	Molten salt
turb	Turbine
st	Steam
p	Pump
cond	Condenser
en	Energy
abs	Absorbed
isen	Isentropic
elect	Electrolyzer

Acronyms

LHV	Low heating value
HTF	Heat transfer fluid
UAE	United Arab Emirates
SOEC	Solid oxide electrolyzer cell
CO_2	Carbon dioxide
H_2	Hydrogen
NaOH	Sodium hydroxide
KOH	Potassium hydroxide
HTSE	High temperature steam electrolysis
VHTR	Very high temperature reactor
ORC	Organic Rankine cycle
PEM	Polymer electrolyte membrane
OTEC	Ocean thermal energy conversion
HRHG	Heat recovery heat generator
HRSG	Heat recovery steam generator
EES	Engineering Equations Solver
THE	High temperature electrolysis
S-I	Sulfur iodine
Cu-Cl	Copper chlorine
SI	System of innovation
LCOE	Localized cost of electricity

technologies, heliostat fields have an operating temperature range of 150-2000°C [1]. High temperature solar collectors are important in large-scale power production and have better efficiency. The flexibility of the operating temperatures in a heliostat field is what makes it the best choice for the application at hand. A heliostat field collector consists of several reflecting mirrors and a tower with a central receiver where molten salt flows and absorbs the heat reflected. The wide field of mirrors focuses the sun's incident rays onto a single receiver to heat up the molten salt. The molten salt then travels through a heat exchanger where heat is lost to the water and high temperature superheated steam is produced. This high temperature steam is then expanded in a steam turbine and electricity is generated.

The cycle responsible for generating electrical power to the electrolyzer is the famous Rankine cycle as shown in Figs. 1 and 2. The cycle consists of a heat exchanger, two steam turbines, a condenser, and a water pump. The efficiency of the Rankine cycle is mainly dependent on the high heat vaporization of the fluid; therefore, for high efficiency of a Rankine cycle, the temperature and pressure of water needs to reach a critical level. The typical entering temperature value at the steam turbine is around 550°C which gives a theoretical maximum Carnot efficiency of around 63% [2]. The molten salt inside the heat exchanger receives the heat in the receiver of the solar collector and gets heated up to a high temperature. This high temperature molten salt transfers the heat to the subcooled water entering the heat exchanger where high temperature steam is generated. The high temperature steam enters the two-stage steam turbines where steam loses energy to produce power. Heat is lost in the condenser cooled by the cooling tower and the cycle is repeated. The power produced by the cycle is used to operate the pumps and the electrolyzer.

As discussed earlier, hydrogen is believed to be the energy carrier of the future. However, hydrogen is not freely available and needs to be produced using existing and renewable sources. Unlike coal which is a

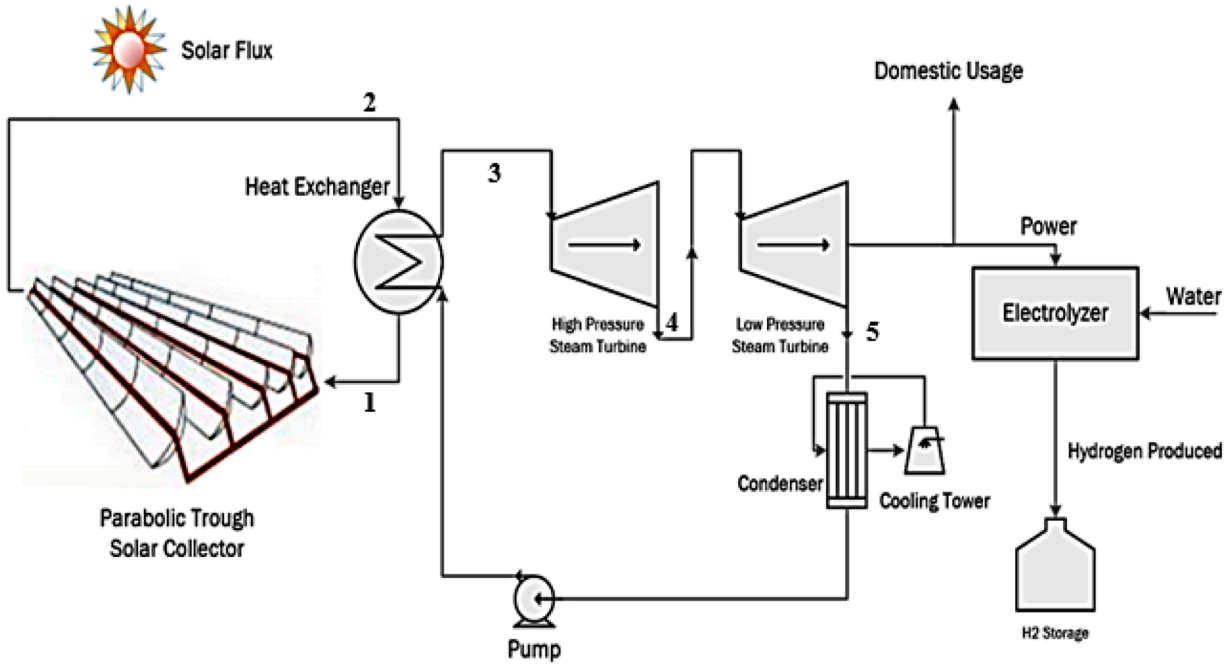

Fig. 1. Overall proposed system with a parabolic trough solar collector.

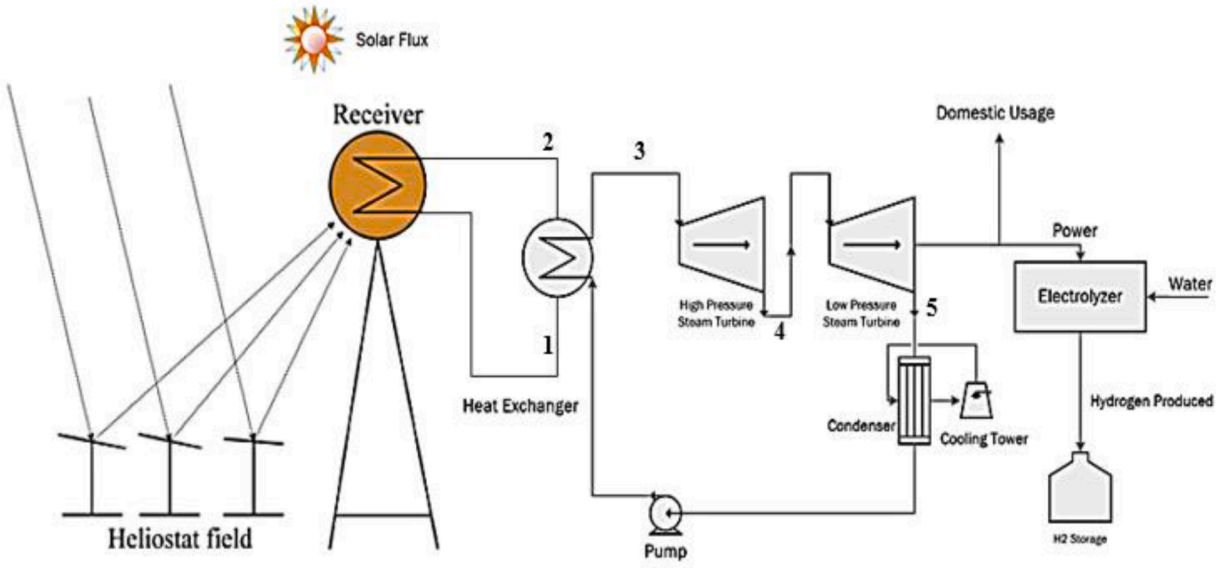

Fig. 2. Overall proposed system with a heliostat field solar collector.

primary energy source, hydrogen serves the same purpose as a battery since it is an energy carrier. The production of hydrogen includes several methods such as steam reformation of hydrocarbons, water electrolysis, and thermochemical splitting of water. Ninety-six percent of the hydrogen produced nowadays is by conventional methods using fossil fuels, whereas the other 4% is produced by water electrolysis.

Thermochemical splitting of water is the most widely covered area in recent research. It uses heat to split water into hydrogen and oxygen molecules, thus producing hydrogen. The heat used in this method can be produced from renewable energy sources such as wind, solar, and geothermal power. It is the most favorable method since renewable sources are expected to contribute even more significantly to the energy supply in the near future.

Steam reformation of hydrocarbons is the production of hydrogen using fuels such as natural gas. This process is carried out in a reformer where fossil fuels react with steam at very high temperatures producing hydrogen and providing it to fuel cells. The issue with this method is that it utilizes hydrocarbons that produce CO_2 emissions upon reaction in the reformer-fuel-cell system. Considering these emissions, global warming issues will arise and the idea of using renewable sources is overlooked.

The most favorable method of hydrogen production, especially considering both renewable energy sources and the Rankine cycle, is the water electrolysis method. Water electrolysis uses electricity generated from a steam turbine where electric current is passed through water and water is decomposed into hydrogen and oxygen. Hydrogen is produced in an electrolyzer cell at the cathode and oxygen at the anode with a power source in between. A tremendous amount of energy is required to break the strong bond between hydrogen and oxygen inside the water molecule; therefore, catalysts such as sodium hydroxide (NaOH) or potassium hydroxide (KOH) are used to loosen the bond. The most

common electrolyzer used in thermal power plants with high temperatures is the solid oxide electrolyzer cell (SOEC).

In water electrolysis, the electricity used to produce hydrogen comes from renewable sources making it more convenient than other production methods [3]. As mentioned before, the electrolyzer used in the system is a solid oxide electrolyzer cell (SOEC) that utilizes high temperature electrolysis (HTE). A SOEC single cell consists of three main layers. The upper layer is the negative fuel electrode made of nickel having good oxide and electron conductivity and a porous structure where the gases can meet and react. The middle layer is an oxide ion-conducting electrolyte that insulates the gas entrapped [4]. The operation temperature of the SOEC is over 1023 K [5]. The modeling of the process phenomena inside the cell is done using planar rectangular SOECs in order to estimate the electric potential and the energy needs of the cell. This type of modeling is used because of the performance-related characteristics of flexibility, easy production, and compactness.

The SOEC has an operating temperature that can be reached using the parabolic and heliostat collectors and uses simple materials that are environmentally friendly and non-hazardous. The most famous high temperature electrolysis is the SOEC designed by Donitz and Erdle in the 1980s [6]. In a SOEC, water acts as a reactant and is supplied to the cathode part of the electrolyzer, where oxygen ions are transported to the anode part through the electrolyte, leaving hydrogen produced at the cathode side [7]. The thermodynamic reaction of electrolysis is shown in the following equations:

$$H_2O \rightarrow H_2 + \frac{1}{2}O_2$$

The reactions at the anode and cathode sides are,

$$H_2O + 2e^- \rightarrow H_2(g) + O^{2-}(\text{Cathode}) \text{ and } O^{2-} \rightarrow \frac{1}{2}O_2(g) + 2e^-(\text{Anode})$$

High temperature electrolysis is favored because it requires low electrical energy at high temperatures and because the electrolysis of water is highly endothermic with increasing temperatures [7]. Hydrogen production from renewable sources allows us to utilize these existing technologies and reduce environmental pollution.

For centralized power, high temperature solar thermal technology is used since it has high power production and higher efficiencies compared to PV or PV/T systems [8]. The Rankine cycle is the most competitive approach to utilizing the sun's energy and producing power. Organic substances and carbon dioxide are used instead of water to make better use of the thermal energy and are hence called the organic Rankine cycle (ORC). Carbon dioxide is the most researched substance to be used in the Rankine cycle since it is non-explosive, non-flammable, and naturally abundant [9]. Moreover, carbon dioxide reaches its supercritical state (7.38 MPa and 31.1°C) easily and has a better temperature profile to match the heat source temperature because there is no isothermal evaporation of these supercritical fluids [10]. Yang et al. [11] proposed a solar-powered-Rankine-based hybrid power generation system consisting of a solar collector, Rankine cycle, a hydrogen production and storage system. Incident solar radiation is collected by means of parabolic trough solar collectors and concentrated on the absorber tubes. The working fluid is evaporated in the absorber tubes and passed through steam turbines for power production. Excess power is then used in the electrolyzer to produce hydrogen and during off-peak conditions the hydrogen stored is used for auxiliary heating. Using meteorological data taken in 1984 by the Space Research Laboratory, the hybrid cycle produced a net power of 7.886 kWh on the 15th of January and 15.41 kWh on the 16th of July. The 15th of January was a sunny and cold winter day, while the 16th of July was a hot summer day with partial clouds in the late morning hours. The proposed system had a cycle efficiency of 14.47% for the 15th of January and 15.08% for the 16th of July. It is also concluded that ideally 39.3 kWh of energy input is needed per kilogram of hydrogen produced, and that it is sufficient that the hydrogen is stored as compressed gas since it loses energy in liquid form due to the liquefaction process.

Hydrogen can be produced using water electrolysis (splitting of water into hydrogen and oxygen) with the aid of electrical energy. There are three types of water electrolysis: solid oxide, alkaline, and polymer electrolyte membrane (PEM) electrolysis [12]. PEM electrolysis is the preferred type of water splitting process because it uses a solid electrolyte membrane that is expected to increase the lifetime of the electrolyzer. The advantages of PEM electrolysis over conventional alkaline electrolysis are that it is a simple, cost effective, and sustainable technology for producing and storing hydrogen [13]. Tinoco et al. [14] investigated high temperature electrolysis which is the most efficient and sustainable process for the production of hydrogen. Since it operates in the auto-thermal mode, it does not require a high-temperature source for the electrolysis but rather an energy source to supply enough heat to vaporize water. The electrolyzer used in the study is Solid Oxide Electrolysis Cells (SOECs) operating at a temperature of over 1023 K. A simplified economic model was used in order to assess the impact of temperature, pressure, and thermal energy cost of the heat source on the process competitiveness. The results showed that the exothermal mode in the electrolyzer cells (high current density) seemed efficient considering the low production cost but in return diminished the lifespan of the cells, leading to a high overall cost of hydrogen production. The study established a hydrogen production cost of $170 per kW electricity produced which certainly shows a low production cost, but the lifespan of the electrolyzer cells is shortened.

Mingyi et al. [15] also performed a thermodynamic analysis on the efficiency of high temperature steam electrolysis (HTSE) with a Solid Oxide Fuel Cell (SOFC). HTSE is the primary energy source as well as the provider of thermal energy to the SOFC, where electrolysis of the high temperature steam takes place, producing hydrogen. Electrical efficiency, electrolysis efficiency, thermal efficiency, and overall efficiency of the system were investigated. The temperature increase from 500 to 1000°C decreased the overall and electrical efficiencies, while increasing the thermal efficiency. The overall efficiency of the system (HTSE) coupled with a solar reactor was calculated to be 59% more than that of the conventional alkaline electrolysis systems at 33%.

Research all over the world shows several configurations of solar system to ensure sustainable hydrogen production and higher efficiencies. High temperature solar thermal technologies are available such as parabolic troughs, heliostat fields, and solar dishes. The operating temperature of these technologies is different and, depending on the system required, each can be used for the production of hydrogen through thermodynamic systems. Parabolic troughs have an operation temperature range of 60-300°C, solar dishes have a range of 100-500°C, and heliostat fields have a range of 150-2000°C [1]. Zhang et al. [16] presented a new solar-driven high temperature steam electrolysis for which energy consumption was studied. The system is composed of a solar concentrating beam splitting system, a Solid Oxide Steam Electrolyzer (SOSE), two heat exchangers, a separator, and storage tanks. Parametric studies were conducted to investigate the effect of current density with the efficiency of the SOSE, showing that the anode-supported SOSE had the best performance as it had the lowest electrical energy requirement. Further parametric analysis was done on the effect of the operating temperature on the efficiency of the SOSE, resulting in a maximum efficiency at a certain operating temperature. The thermal energy and electrical energy distribution from the solar concentrated beam splitting system, which is very important in the optimal design of high temperature electrolysis, was further investigated. The balance parameter, which is the ratio of thermal to electrical energy from the solar collector, and the current density were studied for different operating temperatures. The results showed an increase in the balance parameter with a decreasing operating temperature, but the effects are comparatively small at a lower and higher current density. It is concluded in this study that the thermal and electrical energy should be distributed reasonably for the optimum operation of the SOSE with

the solar concentrated beam splitting system.

Several renewable energy sources can be implemented in the design of a hydrogen production system. Dincer and Ratlamwala [17] discuss five renewable energy systems based on hydrogen production systems in a comparative study showing the advantages and disadvantages of each in terms of energy efficiency. In another study by Ahmadi et al. [18] energy and exergy analysis was presented for hydrogen production by ocean thermal energy conversion (OTEC) coupled with a proton exchange membrane electrolyzer (PEM). The system in this study consists of a flat solar collector, a turbine, an evaporator, and a PEM electrolyzer. Warm surface seawater is used to evaporate a working fluid (ammonia or freon), driving a turbine to produce electrical power which is then used to drive the PEM electrolyzer to produce hydrogen. The cycle for power production is an organic Rankine cycle and is used in the energy and exergy analysis. The results of the system's analysis show an exergy efficiency of 22.7%. This result shows that any increase in solar radiation intensity increases the exergy efficiency and hydrogen production rate. The ambient temperature, on the other hand, decreases the exergy efficiency and the sustainability index when below 298 K, but increases the exergy efficiency and sustainability index when above 298 K.

Moreover, Al Zaharani et al. [3] proposed an integrated system for power, hydrogen, and heat production utilizing geothermal energy. The proposed system consists of a supercritical carbon dioxide Rankine cycle cascaded by an organic Rankine cycle (ORC) coupled with an electrolyzer and heat recovery system. The power output from the Rankine cycle is used to drive the electrolyzer, and the thermal energy output is utilized for space heating. The results of the thermodynamic analysis (energy and exergy analysis) show the capability of the proposed system to produce 245 kg/h of hydrogen for a net power output of 18.59 MW used in the electrolyzer. The overall energy and exergy efficiencies are 13.37% and 32.27% respectively, with a total exergetic effectiveness of 43.22%. Also, the results show that increasing the temperature of the geothermal source leads to an increase in the overall exergetic efficiency of the system.

Ozturk and Dincer [19] similarly performed a thermodynamic analysis on a multigeneration plant producing power, heating, cooling, hot water, and hydrogen. The system consisted of four parts: a Rankine cycle sub-system, an organic Rankine cycle sub-system, a hydrogen production sub-system, an absorption and cooling sub-system, and a hydrogen utilization sub-system. The hydrogen production sub-system utilizes high temperature steam electrolysis (HTSE) where power is needed in terms of electricity and thermal heat. The absorption sub-system is used instead of a conventional refrigeration system to utilize surplus heat in the system. The overall thermal energy and exergy efficiencies of the system were found to be 52.71% and 57.35% respectively, having a large amount of heat recovery within the system since the sub-system efficiencies were lower. The results also showed the largest exergy destruction of on average 17% in the parabolic trough solar collector mainly due to the high temperature difference between the working fluid going into the collector and the surface temperature of the receiver tubes. Finally, a parametric analysis showed that the increase in solar flux and collector receiver temperature increased the exergy efficiency.

A plant is designed to supply the required energy for the hydrogen production process along with the electrical energy generation proposed by Burulay et al. [20]. In the study, a solar energy power plant integrated with a biomass-based hydrogen production system is investigated. Results show that designing and operating a hybrid high-performance energy system using two different renewable sources is an encouraging approach to reduce the environmental impact of energy conversion processes and the effective use of energy resources.

Qureshy and Dincer [21] developed a new renewable energy-based cogeneration system for hydrogen and electricity production. Three different methods for hydrogen production are integrated with Rankine cycle for electricity production using solar energy as an energy source. A thermodynamic modeling and assessment of the solar-based integrated energy systems for hydrogen production with and without thermoelectric generators waste heat recovery system presented by Khanmohammadi and Targhi [22]. They observed a higher increase in efficiency in their proposed system, whereas the variations of efficiency relative to the mass flow rate of the collector are extremely slight in the conventional system.

Yilmaz et al. [23] designed a new solar power assisted multigeneration system to perform heating, cooling, drying, hydrogen and power generation with a single energy input. The proposed study consists of seven sub-parts which are namely parabolic dish solar collector, Rankine cycle, organic Rankine cycle, PEM-electrolyzer, double effect absorption cooling, dryer and heat pump. Sadeghi and Ghandehariun [24] presented a thermodynamic analysis of solar-based hydrogen production via copper chlorine (Cu-Cl) thermochemical water splitting cycle. The integrated system utilizes air as the heat transfer fluid of a cavity-pressurized solar power tower to supply heat to the Cu-Cl cycle reactors and heat exchangers. Atiz et al. [25] investigated power and hydrogen production performance of an integrated system. The system consists of an organic Rankine cycle, parabolic trough solar collectors having a surface area of 545 m^2, middle-grade geothermal source, cooling tower and proton exchange membrane. As a result, the energy and exergy efficiency is calculated to be 5.85% and 8.27%, respectively. A new integrated energy system using a renewable energy source is developed to generate hydrogen in a clean manner and a complete thermodynamic analysis and assessment through energy and exergy approaches for the solar-water-hydrogen-power cycle is carried out by Qureshy and Dincer [26]. The presented results show that the proposed system achieves a 25.07% of energy efficiency and a 31.01% of exergy efficiency, respectively. Yand et al. [27] focused on exploring a universal method for determining the power reallocation and capacity configuration for a grid-connected PV power station integrated hydrogen production system.

In this study, we propose a model that integrates a solar harvesting system into a conventional Rankine cycle, producing electrical and thermal power used in domestic applications, and generating hydrogen by high temperature electrolysis (HTE) using a solid oxide steam electrolyzer (SOSE). The model is divided into three subsystems: the solar collector(s), the steam cycle, and an electrolysis subsystem. In addition, the two types of solar collectors are utilized, namely, heliostat field collectors, and parabolic trough collectors. Combining all of these systems facilitate cogeneration of electrical and thermal power, as well as the production of hydrogen which serves as an effective energy source for use in diverse applications. With regards to the solar collector selection, heliostat fields and parabolic trough collectors are two of the most commonly utilized solar thermal collectors. Therefore, investigating these two collectors helps shed light on the practicality of their implementation and the optimum conditions under which both systems operate. The objective of this research is to carry out a thermodynamic analysis on each subsystem along with the overall proposed model to evaluate their performance and determine which system exhibits superior performance. The systems are further analyzed by conducting a parametric study to investigate the performance of the system and the rate of hydrogen produced under different conditions such as varying the solar flux and the area of the solar collector. A direct search method optimization techniques embedded in ESS is utilized to determine optimum operating conditions that can yield maximum performance of both systems.

2. System description

Figs. 1 and 2 show the schematic diagram of the solar collectors (parabolic trough and heliostat field) integrated with a Rankine cycle. Both of the proposed systems utilize concentrated solar collectors with receivers carrying a heat transfer fluid (HTF), which is molten salt in the heliostat central receiver and Therminol VP-1 in the parabolic trough receiver. The molten salt contains 60% $NaNO_3$ and 40% KNO_3 [28]. The

first schematic diagram shows the parabolic solar trough coupled with a Rankine cycle producing a net power output to run the electrolyzer for hydrogen production. The second schematic diagram differs in the solar collector part where a heliostat field is used.

For the proposed system, a particular location is needed in order to extract the global solar radiations to be used as an initial assumption for solar energy. The location that will be used is Abu Dhabi (24.43°N, 54.45°E), since the solar radiation in the UAE is very high. The solar radiation for Abu Dhabi is shown in Table 1 [27].

The overall system can be studied as four sub-systems: the solar collector sub-system, the thermal heat exchanger, the Rankine cycle, and the electrolyzer. The first sub-system will be analyzed using two different solar collectors: the parabolic trough and the heliostat field solar collector. The parabolic trough solar collector reflects the heat coming from the sun (solar flux) using a parabolic-shaped mirror onto a vacuum-sealed pipe where the HTF (Therminol VP-1) is heated up to high temperatures. Similarly, the heliostat field uses a number of projected mirrors to reflect the sun's rays onto a central receiver achieving higher temperatures of molten salt. The high temperature HTF then passes through the heat exchanger, typically in a counter flow mode, and the heat is transferred to the water in the Rankine cycle where superheated steam is generated. The superheated steam is then expanded in the two-stage steam turbine generating shaft work, which is then converted to electrical power using the electrical generator.

3. Analysis

A thermodynamic analysis in terms of energy and exergy is presented for each component of each subsystem. Also, heat transfer of both parabolic trough and heliostat field collectors is studied to evaluate the heat losses and heat absorbed inside each of the receivers. In this regard, temperatures of the receiver cover, heat transfer fluid temperature, thermal efficiency, and useful energy in the receiver are determined. These analyses are carried out in order to have a better understanding of the optimum collector to use. The efficiency of a solar collector depends mainly on the inlet temperature, outlet temperature, ambient temperature, and wind speed.

Assuming a steady state with no pressure change, the parabolic collector's useful energy output is defined as [29],

$$\dot{Q}_u = \dot{m}_r(Cp_{ro}T_{r0} - Cp_{ri}T_{ri}) \tag{1}$$

where, $\dot{m}_r$ is the mass flow rate in the receiver, Cp is the specific heat, and T is the temperature. The subscripts ro and ri refer to the receiver's inlet and outlet. The useful energy can also be calculated as,

$$\dot{Q}_u = A_{ap}F_R\left(S - \frac{A_r}{A_{ap}}U_L(T_{ri} - T_o)\right) \tag{2}$$

where, A_{ap} is the receiver area, F_R is the heat removal factor, S is the heat absorbed by the receiver, and U_L is the solar collector overall heat loss coefficient. The heat absorbed by the receiver is,

$$S = G_b\eta_r \tag{3}$$

Therefore, the amount of solar radiation that is reflected on the collector and is a heat input into the system is defined by,

$$\dot{Q}_{solar} = A_{ap}F_RSCol_rCol_s \tag{4}$$

where, Col_r and Col_s are the total number of solar collector modules in rows and in series, respectively. The thermal efficiency of the parabolic solar collector is therefore written as,

$$\eta_{c,th} = \frac{\dot{Q}_u}{G_bA_{ap}} \tag{5}$$

Table 1
Global solar radiation in Abu Dhabi, all in W/m^2.

Highest daily solar radiation	369
Monthly mean solar radiation	290
Highest one-minute average in one day	1041

High temperature solar collectors are important in larger power production and efficiency. The flexibility of the operating temperatures in a heliostat field is what makes it the best choice for the application at hand. The receiver of the heliostat field is coupled with a heat exchanger with molten salt to transfer the heat to the working fluid of the Rankine cycle (i.e. water) [30]. The molten salt is a mixture of 60 wt% $NaNO_3$ and 40 wt% KNO_3 [28]. The density (ρ), specific heat (c_p) and thermal conductivity (λ) of molten salt are given [28] in terms of temperature as; $\rho = 2090 - 0.636 \times T(^\circ C)$, $c_p = 1443 + 0.172 \times T(^\circ C)$ and $\lambda = 0.443 + 1.9 \times 10^{-4} \times T(^\circ C)$, respectively.

For the heliostat filed, the rate of heat received by the solar irradiation is calculated as [17],

$$\dot{Q}_s = I \times A_{field} \tag{6}$$

where, I represents the region's solar light intensity and A_{field} represents the area of the heliostat field. The rate of heat received by the central receiver is,

$$\eta_H = \frac{\dot{Q}_{rec}}{\dot{Q}_s} \tag{7}$$

Also, the rate of heat absorbed by the molten salt passing through the central receiver is,

$$\dot{Q}_{rec,abs} = \dot{m}_{ms} \times c_p \times \left(T_{ms,o} - T_{ms,in}\right) \tag{8}$$

where, $\dot{m}_{ms}$ is the mass flow rate of the molten salt, c_p is the specific heat capacity of the molten salt, and $T_{ms,o}$&$T_{ms,in}$ are the temperatures of the molten salt entering and leaving the receiver, respectively. Therefore, the total heat received by the receiver is calculated as follows:

$$\dot{Q}_{rec} = \dot{Q}_{rec,em} + \dot{Q}_{rec,ref} + \dot{Q}_{rec,conv} + \dot{Q}_{rec,cond} + \dot{Q}_{rec,abs} \tag{9}$$

where, the heat losses occurring inside the receiver are by emissive, reflective, convective, and conductive means. The temperature of the central receiver of heliostat field is calculated as,

$$\frac{\dot{Q}_{rec}}{\frac{A_{field}}{F_rC}} = \frac{T_{rec,surf} - T_{ms}}{\frac{d_o}{d_oh_{ms}} + d_o\left(\frac{\ln\left(\frac{d_o}{d_i}\right)}{2\lambda_{tube}}\right)} \tag{10}$$

where, d_o & d_i both represent the outer and inner diameters of the absorber tube, T_{ms} represents the average temperature of the molten salt, λ_{tube} represents the conductivity of the absorber tube, and h_{ms} represents the convective heat transfer coefficient. The thermal energy efficiency of the heliostat field receiver is defined as,

$$\eta_{en} = \frac{\dot{Q}_{rec,abs}}{\dot{Q}_{rec}} \tag{11}$$

The energy equations to model the Rankine cycle in the solar power conversion of steam are as follow. The power generated by the turbine is calculated as [30],

$$\dot{W}_{turb} = \dot{m}_{st}(h_3 - h_4) + \dot{m}_{st}(h_4 - h_5) \tag{12}$$

The enthalpies of state 4 and state 5 are calculated from the turbine isentropic efficiencies as,

$$\eta_{turb} = \frac{h_3 - h_4}{h_3 - h_{4s}} \tag{13}$$

and

$$\eta_{turb} = \frac{h_4 - h_5}{h_4 - h_{5s}} \tag{14}$$

The power needed by the water pump is expressed as,

$$\dot{W}_p = \dot{m}_{st}(h_2 - h_1) \tag{15}$$

The actual power produced from the steam cycle is,

$$\dot{W}_{net} = \dot{W}_{turb} - \dot{W}_p - \dot{W}_{parasitic} \tag{16}$$

The parasitic losses are used for a more realistic model to account for losses occurring in the system. A 10% loss is assumed and calculated as,

$$\dot{W}_{parasitic} = 0.1\left(\dot{W}_{turb} - \dot{W}_p\right) \tag{17}$$

The rate of heat rejected by the condenser is calculated as,

$$\dot{Q}_{cond} = \dot{m}_{st}(h_5 - h_1) \tag{18}$$

The energy efficiency of the steam cycle is defined as,

$$\eta_{en} = \frac{\dot{W}_{net}}{\dot{Q}_{rec,abs}} \tag{19}$$

The rate of hydrogen produced is calculated using the electrical conversion efficiency of the electrolyzer given as [17],

$$\eta_{electrolyzer} = \frac{\dot{m}_{H_2} LHV}{\dot{W}_{net}} \tag{20}$$

where, the efficiency of the electrolyzer is estimated as 70% and the LHV of hydrogen as 191.2 MJ/kg [3].

4. Results and discussion

It is important to note that, the developed mathematical and thermodynamic analyses were verified in a previous study by the same authors in [31], where the obtained results were within an acceptable margin of error. The performance of the overall system when using both parabolic trough and heliostat field solar collectors is studied with the variation of different independent parameters. The variation of solar irradiation on the thermal efficiency of each sub-system and the overall system is shown in Fig. 3 together with the effect on the mass flow rate of hydrogen produced at the electrolyzer. The solar flux is increased from 300 to 1100 W/m^2 at which the thermal efficiency of the parabolic trough increases very slightly starting from 71% and the heliostat field efficiency also rises marginally starting from 92%. The thermal efficiency of the Rankine cycle increases from 31% to 37% when using the parabolic trough and from 33% to 43% when using the heliostat field solar collector. Additionally, the overall thermal efficiency of the whole system increases from 15% at 300 W/m^2 to 17% at 1100 W/m^2 when using the parabolic trough whereas the overall efficiency increases from 21% to 27% when using the heliostat field solar collector. The increase in the overall thermal efficiency is very small as increasing the solar irradiation has no effect on the efficiency of the collectors but slightly rises the efficiency of the Rankine cycle because of the increased temperature of the molten salt in the receiver due to high solar incident. On the other hand, since the efficiency of the Rankine cycle goes up with the increase in solar flux, the amount of hydrogen produced also increases due to the fact that the net power output goes up. The increase in hydrogen production rate is from 0.053 kg/s at 300 W/m^2 to 0.087 kg/s at 1100 W/m^2 when using the parabolic trough collector. Using the heliostat field solar collector increases the hydrogen production rate from 0.063 kg/s at 300 W/m^2 to around 0.125 kg/s at 1100 W/m^2. As a result, higher hydrogen production is achieved using the heliostat field but at the price of higher running and initial costs since heliostat fields are very sensitive to changes in operation variables and the direction of the sun, unlike parabolic troughs where sun tracking technologies are present and working effectively.

The effect of the aperture area on the thermal efficiency of the overall efficiency considering each sub-system and the effect on hydrogen production rate when using the parabolic trough are shown in Fig. 4. Upon increasing the aperture area of the parabolic trough from 10 m^2 to 80 m^2, the efficiency of each sub-system increases, leading to an increase in the efficiency of the overall system. The efficiency of the parabolic trough is almost constant with the increase in the aperture area as discussed in the analysis of the parabolic trough. However, the efficiency of the Rankine cycle increases slightly from 35% at a 10 m^2 aperture area to 40% at an 80 m^2 area. This increase in the thermal efficiency of the Rankine cycle leads to an increase in the overall efficiency of the whole system from 16% to 20% with the increase in the aperture area. Moreover, the increase of the aperture area from 10 m^2 to 80 m^2 leads to an increase in the hydrogen production rate from 0.0775 kg/s at 10 m^2 to

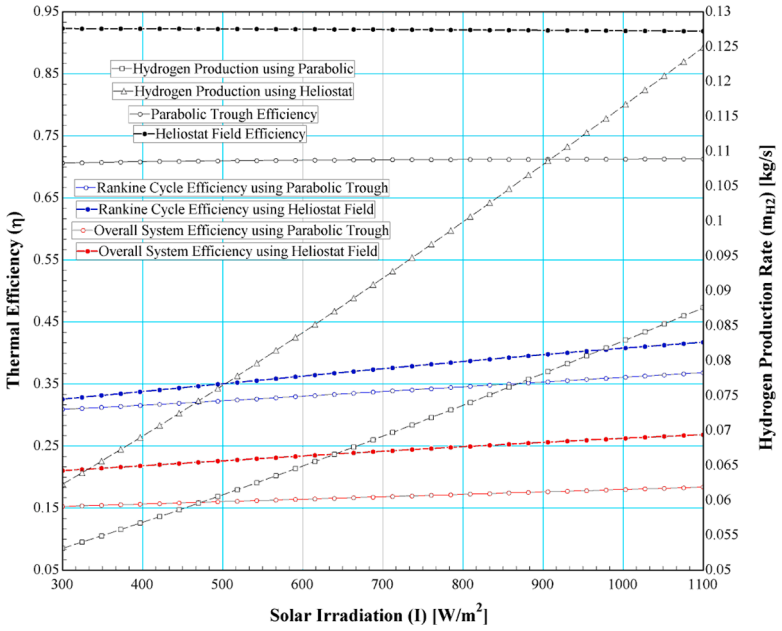

Fig. 3. Effect of the solar flux on the thermal efficiency of each sub-system and the overall system and on the rate of hydrogen produced with both parabolic trough and heliostat field collectors.

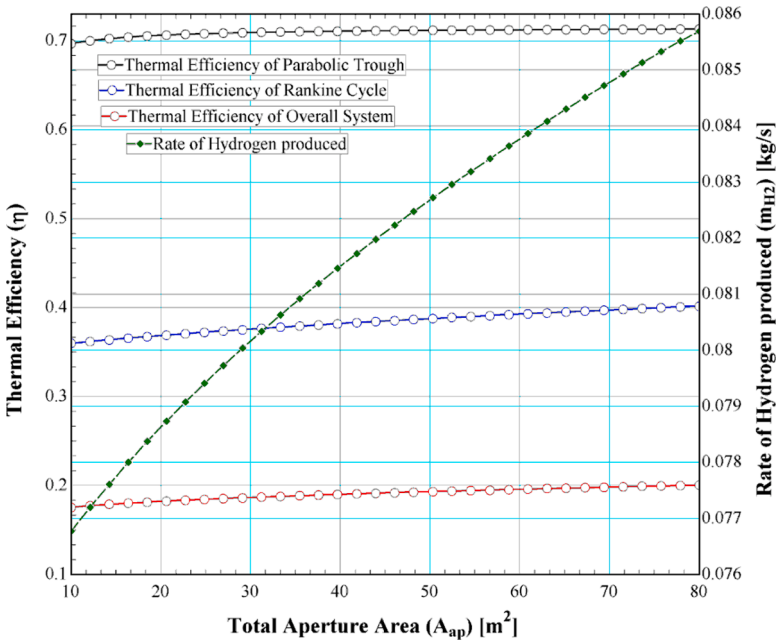

Fig. 4. Effect of the parabolic trough aperture area on the thermal efficiency of each sub-system and the overall system and on the rate of hydrogen produced.

0.086 kg/s at 80 m^2 aperture areas, which is considered a slight but acceptable increase in mass flow rate.

Fig. 5 shows the effect of increasing the mass flow rate of the molten salt in the parabolic trough receiver (HTF) on the thermal efficiency of the whole system considering the overall system and the effect on the hydrogen production rate. As the mass flow rate is increased from 5 kg/s to 15 kg/s, the thermal efficiency of the parabolic trough increases slightly from 68% to 73% which shows the little effect of the mass flow rate on the performance of the parabolic trough. As for the Rankine cycle, the thermal efficiency increases from 29% to 47% at a mass flow rate of 15 kg/s. This is due to the fact that increasing the mass flow rate of the HTF will result in increased inlet temperature at the turbine, since the counter flow heat exchanger enables the heat transfer from the HTF to the water, and increasing either mass flow rates will increase the inlet temperature to the two-stage turbine. The overall system efficiency will therefore increase from 14% at 5 kg/s to 25% at 5 kg/s since a higher net power output is produced at the turbine in the Rankine cycle, increasing the overall thermal efficiency. The effect on the hydrogen production rate is showing a significant increase from 0.04 kg/s at a 5 kg/s flow rate of HTF to 0.21 kg/s of hydrogen flow rate at 15 kg/s of HTF mass flow rate. The increase in hydrogen production is due to the fact that a higher net power output is produced by the Rankine cycle; therefore, the electrolyzer output will yield higher hydrogen production as a result. Of course, there is a limit to increasing the mass flow rate of the HTF inside the receiver's tube due to material design and heat transfer effectiveness.

Fig. 6 shows that the heliostat field area is an independent variable that can be increased or decreased to increase the performance of the

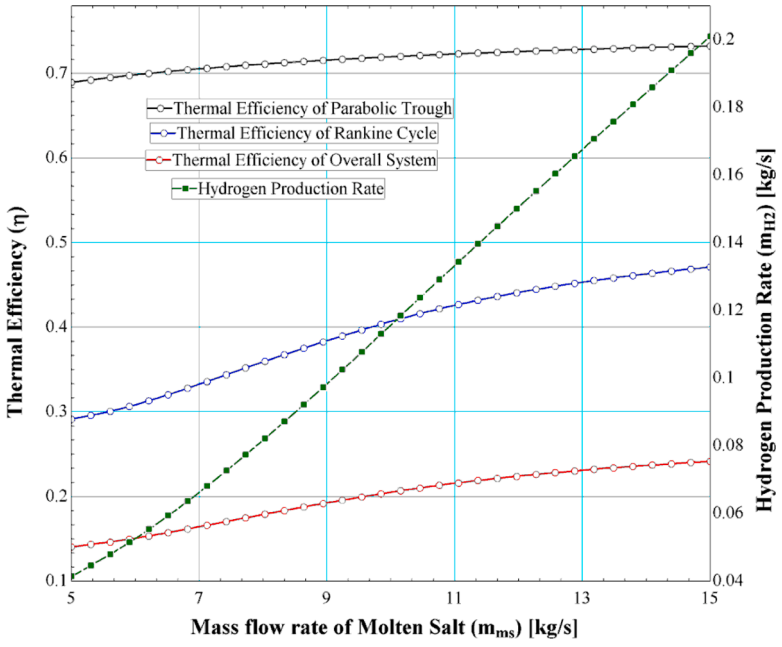

Fig. 5. Effect of the molten salt mass flow rate in the parabolic trough receiver on the thermal efficiency of each sub-system and the rate of hydrogen produced.

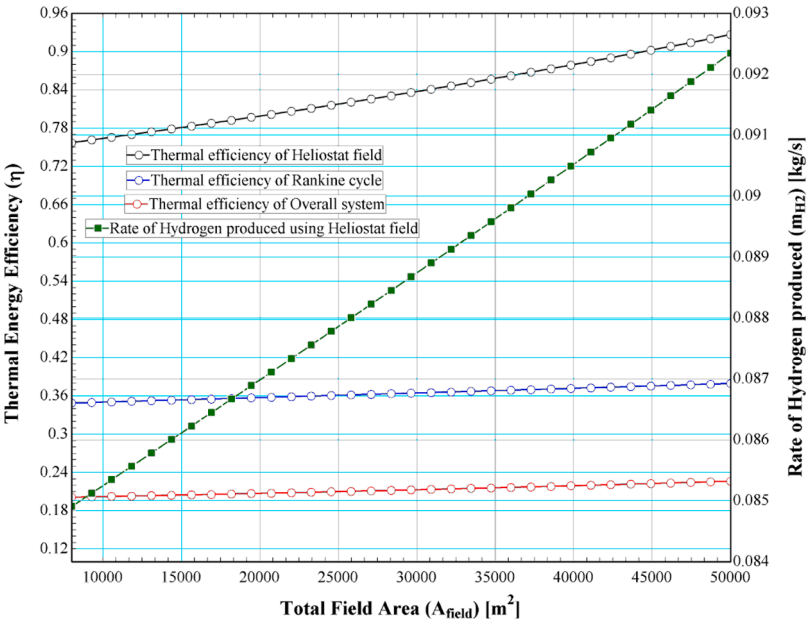

Fig. 6. Effect of the heliostat field area on the thermal efficiency of each sub-system and the rate of hydrogen produced.

overall system. Upon increasing the heliostat field area from 10000 m^2 to 50000 m^2, the thermal efficiency of the heliostat field increases from 76% to 92%, which is a significant increase considering that the increase in the area of the field means more sun rays are reflected onto the central receiver as a percentage of the incoming solar incident, and in return the efficiency is much improved. Increasing the total field area also increases the thermal efficiency of the Rankine cycle but by a negligible amount; the increase is from 35% to 38%. With that, the overall thermal efficiency of the whole system increases accordingly from 20% at 10000 m^2 of the heliostat field area to 23% at 50000 m^2 of the heliostat field area. The increase in hydrogen production is not that significant either as the hydrogen mass flow rate is 0.085 kg/s at 10000 m^2 and increases to 0.0924 kg/s at 50000 m^2. The reason is that the heliostat field uses several reflector mirrors to concentrate the solar incident onto one point (central receiver), and increasing the field area, which means increasing the number of reflective mirrors, does not increase the temperature of the molten salt inside the receiver by a large amount. This is because a small heliostat field area (10000 m^2) can reach the operating temperatures of the heliostat collector (1000°C) at the central receiver since it is optimized to reach those temperatures.

As discussed before, the concentration ratio describes the concentration of light rays onto the central receiver. If the concentration number is high, then the heliostat field is effective. Increasing the concentration ratio from 300 to 1400 increases the thermal efficiency of the heliostat field from 76% to 92% expectedly since the mirrors are more effective optically to concentrate the solar incident onto the central receiver of the heliostat field, increasing the heat absorbed by the molten salt, and hence increasing the thermal efficiency. The increase in thermal efficiency of the heliostat field is very rapid when the concentration ratio is increased from 300 to 900 since the efficiency change is 15% as compared to increasing the concentration ratio from 900 to 1400 where the increase in efficiency is only 2%. The Rankine cycle thermal efficiency also increases from 23% to 41% since the temperature of the molten salt increases with the increase in heat absorption by the receiver which in turn increases the temperature at the turbine inlet when the counter flow heat exchanger dissipates the heat to the water converting it to superheated steam at the turbine inlet. With the increase in temperature at the turbine inlet, the net power output also increases which results in an increase of thermal efficiency of the steam cycle. Additionally, the overall thermal efficiency of the system also increases from 12% to 27% when the concentration ratio is increased from 300 to 1400. The results are presented in Fig. 7.

As seen from Fig. 8, the increase in the outlet temperature of the molten salt in the heliostat receiver increases the thermal efficiency of the collector field from 72% at 630 K temperature of molten salt to 92% at 790 K molten salt temperature. The increase in thermal efficiency is very rapid when the temperature is increased from 630 K to around 710 K since the increase in efficiency is 18% for an 80 K increase in molten salt temperature. The thermal efficiency of the Rankine cycle also increases from a very low 12% at a temperature of 630 K to 40% when a high temperature of around 790 K is achieved. The increase in thermal efficiency of the Rankine cycle is not limited to 790 K since increasing the molten salt temperature further yields a greater increase in the efficiency of the Rankine cycle. The maximum temperature of molten salt that can be achieved depends on the other heliostat geometric variables, the mass flow rate of molten salt, and the solar flux acting on the field. In the subsequent optimization section, the best high temperature of molten salt will yield a higher thermal efficiency of the Rankine cycle of more than 40%. With the increase in both the heliostat field and Rankine cycle efficiencies, the overall thermal efficiency of the system also increases from a very low 8% due to the low molten temperature, to 27% at a temperature of 790 K. Higher molten temperatures will result in even higher thermal efficiency for the overall system and hence more hydrogen production at the electrolyzer. The hydrogen production rate also increases accordingly with the increase in molten salt temperature from 0.003 kg/s to 0.135 kg/s. The mass flow rate of hydrogen produced at the higher temperatures can also increase due to the fact that the inlet temperature at the turbine will be high, resulting in a higher net power output and producing a higher hydrogen mass flow rate.

Table 2 highlights the independent parameters that have been used for optimization, whereas Tables 3 and 4 show the optimized results for energy efficiency and hydrogen production at the electrolyzer. The Direct Search method inside EES is used for the optimization by varying the incident solar flux, turbine pressures, heliostat field area, ambient conditions, mass flow rate of steam, mass flow rate of heat transfer fluid, and molten salt outlet temperature.

The maximum rate of hydrogen produced is 0.3322 kg/s as optimized in EES, and the highest overall thermal efficiency is 25.35% for the parabolic trough solar collector. On the other hand, the maximum overall thermal efficiency when using the heliostat field is 27%, and the maximum hydrogen production rate is 0.411 kg/s.

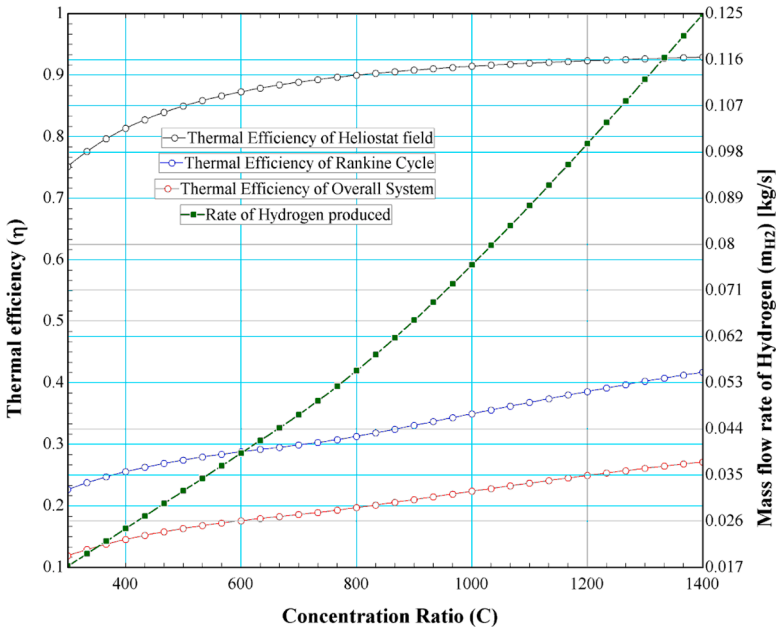

Fig. 7. Effect of the heliostat field concentration ratio on the thermal efficiency of each sub-system and the rate of hydrogen produced.

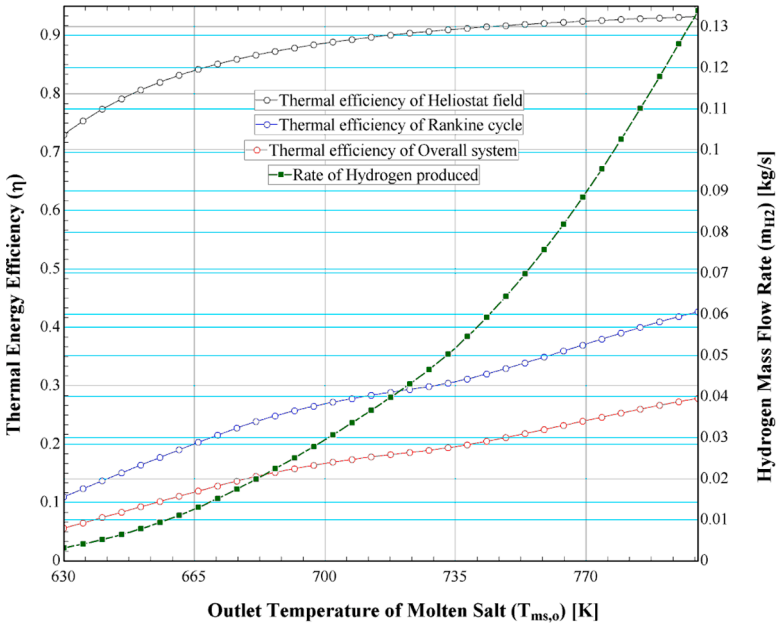

Fig. 8. Effect of the molten salt outlet temperature in the heliostat field receiver on the thermal efficiency of each sub-system and the rate of hydrogen produced.

Table 2
Independent parameters used for optimization.

Parameter	
I	300-1100 [W/m^2]
A_{ap}	10-80 [m^2]
A_{field}	10,000-50,000 [m^2]
C	300-1400
$\dot{m}_{ms}$	5-15 [kg/s]
$\dot{m}_s$	0.4-1 [kg/s]
P_3	1-12 [MPa]
P_4	1-12 [MPa]
$T_{ms,i}$	300-400 [K]
$T_{ms,o}$	630-1000 [K]

Table 3
Optimized results for overall thermal efficiency.

Parameter	Parabolic Trough Collector	Heliostat Field Collector
I	1100 [W/m^2]	1100 [W/m^2]
A_{ap}	80 [m^2]	A_{field} = 50000 [m^2]
P_3	12 [MPa]	5 [MPa]
P_4	1 [MPa]	4.5 [MPa]
$\dot{m}_s$	0.4 [kg/s]	0.4 [kg/s]
$\dot{m}_{ms}$	7.4 [kg/s]	7.4 [kg/s]
$T_{ms,i}$	300 [K]	400 [K]
$T_{ms,o}$	800 [K]	980 [K]
$\eta_{overall}$	25.35 %	27 %

Table 4
Optimized results for the amount of hydrogen produced.

Parameter	Parabolic Trough Collector	Heliostat Field Collector
I	804 [W/m^2]	1000 [W/m^2]
A_{ap}	53 [m^2]	A_{field} = 50000 [m^2]
P_3	12 [MPa]	12 [MPa]
P_4	1 [MPa]	1 [MPa]
$\dot{m}_s$	0.756 [kg/s]	0.8 [kg/s]
$\dot{m}_{ms}$	15 [kg/s]	10 [kg/s]
$T_{ms,i}$	300 [K]	300 [K]
$T_{ms,o}$	800 [K]	1000 [K]
$\mathbf{m_{H2}}$	0.3322 [kg/s]	0.411 [kg/s]

5. Conclusions

The energy and exergy analysis carried out in the section above allows us to draw the following conclusions:

- Thermal efficiencies for the parabolic trough range from 50% to 73%, with the latter achieved at a high mass flow rate of molten salt of 20 kg/s and the highest solar incident of 1100 W/m^2.
- The thermal efficiency of the heliostat field ranges from 74% to 92%. Higher solar incident and high concentration ratio achieve a maximum efficiency of 90%. Using a total field area of 50000 m^2, the energy efficiency of the heliostat collector reaches 92%.
- The maximum efficiency obtained from the Rankine cycle is around 45% using a steam mass flow rate of 15 kg/s. Of course, the piping size and materials will limit the mass flow rate, the optimized value of which it absorbs all the heat from the molten salt in the heat exchanger.
- The overall system efficiency is highest at 27% when using the heliostat field, which is considered low. Thermal power plants using solar energy tend to have lower efficiencies, but at the same time they produce zero greenhouse gas emissions and thus contribute to a cleaner environment.
- The hydrogen production rate reaches a maximum of 0.411 kg/s or 24.56 kg/h when using the heliostat field, with the incident irradiation at its maximum and the highest mass flow rate of molten salt.
- The outlet temperature of molten salt increases as long as the receiver absorbs more heat energy. The increase in temperature means a higher inlet turbine temperature, which in turn increases the power output and therefore results in a higher mass flow rate of hydrogen produced.
- The hydrogen that is not used right away can be stored using thermal storage technologies.
- Underground storage for hydrogen in salt caverns or in depleted oil and gas reservoirs is a good solution for large-scale storage.
- The use of a reheat system between the two-stage turbines increases the net power output and therefore the hydrogen production as well.
- Open-feed water heaters could lead to an increased thermal efficiency, producing more net electricity and hence a higher mass flow rate of hydrogen.
- Heliostat field collectors are a proven solution for higher overall efficiency and have the highest hydrogen production flow rate at 0.2 kg/s.
- The efficiency of the electrolyzer used was 70%. The option of choosing a more efficient electrolyzer will result in the production of more hydrogen.
- The mass flow rate of water to the electrolyzer for molecule-level breakdown is kept constant and was not included in the analysis.

Declaration of Competing Interest

The authors declare that they have no known competing financial interests or personal relationships that could have appeared to influence the work reported in this paper.

Data availability

No data was used for the research described in the article.

References

[1] S.A. Kalogirou, Solar thermal collectors and applications, Progress in Energy and Combustion Sci. 30 (2004) 231–295.
[2] WR B. Stine, W. Harrigan, Power cycles for electricity generation, in: M. Geyer (Ed.), Power From the Sun, John Wiley and Sons, Inc., 1986.
[3] A.A. AlZaharani, I. Dincer, G.F. Naterer, Performance evaluation of a geothermal based integrated system for power, hydrogen and heat generation, Int. J. Hydrogen Energy 38 (2013) 14505–14511.
[4] Y. Bo, Z. Wenqiang, X. Jingming, C. Jing, Status and research of highly efficient hydrogen production through high temperature steam electrolysis at INET, Int. J. Hydrogen Energy 35 (2010) 2829–2835.
[5] C. M. Stoots, J. E. O'Brien, M. G. McKellar, G. L. Hawkes, and S. Herring, "Engineering process model for high-temperature electrolysis system performance evaluation," 2005.
[6] W. Dönitz, E. Erdle, High-temperature electrolysis of water vapor—status of development and perspectives for application, Int. J. Hydrogen Energy 10 (1985) 291–295.
[7] M.A. Laguna-Bercero, Recent advances in high temperature electrolysis using solid oxide fuel cells: a review, J. Power Sources 203 (2012) 4–16.
[8] I. Dincer, T.A.H. Ratlamwala, Development of novel renewable energy based hydrogen production systems: a comparative study, Energy Conversion and Manag. 72 (2013) 77–87.
[9] Y. Chen, P. Lundqvist, A. Johansson, P. Platell, A comparative study of the carbon dioxide transcritical power cycle compared with an organic rankine cycle with R123 as working fluid in waste heat recovery, Appl. Therm. Eng. 26 (2006) 2142–2147.
[10] X.R. Zhang, H. Yamaguchi, An experimental study on evacuated tube solar collector using supercritical CO2, Appl. Therm. Eng. 28 (2008) 1225–1233.
[11] W.J. Yang, C.H. Kuo, O. Aydin, A hybrid power generation system: solar-driven Rankine engine-hydrogen storage, Int. J. Energy Res. 25 (2001) 1107–1125.
[12] D. Shapiro, J. Duffy, M. Kimble, M. Pien, Solar-powered regenerative PEM electrolyzer/fuel cell system, Solar Energy 79 (2005) 544–550.
[13] Ö.F. Selamet, F. Becerikli, M.D. Mat, Y. Kaplan, Development and testing of a highly efficient proton exchange membrane (PEM) electrolyzer stack, Int. J. Hydrogen Energy 36 (2011) 11480–11487.
[14] R. Rivera-Tinoco, C. Mansilla, C. Bouallou, Competitiveness of hydrogen production by high temperature electrolysis: Impact of the heat source and identification of key parameters to achieve low production costs, Energy Conversion and Manag. 51 (2010) 2623–2634.
[15] L. Mingyi, Y. Bo, X. Jingming, C. Jing, Thermodynamic analysis of the efficiency of high-temperature steam electrolysis system for hydrogen production, J. Power Sources 177 (2008) 493–499.
[16] H. Zhang, S. Su, X. Chen, G. Lin, J. Chen, Configuration design and performance optimum analysis of a solar-driven high temperature steam electrolysis system for hydrogen production, Int. J. Hydrogen Energy 38 (2013) 4298–4307.
[17] T.A.H. Ratlamwala, I. Dincer, M. Aydin, Energy and exergy analyses and optimization study of an integrated solar heliostat field system for hydrogen production, Int. J. Hydrogen Energy 37 (2012) 18704–18712.
[18] P. Ahmadi, I. Dincer, M.A. Rosen, Energy and exergy analyses of hydrogen production via solar-boosted ocean thermal energy conversion and PEM electrolysis, Int. J. Hydrogen Energy 38 (2013) 1795–1805.
[19] M. Ozturk, I. Dincer, Thermodynamic analysis of a solar-based multi-generation system with hydrogen production, Appl. Therm. Eng. 51 (2013) 1235–1244.
[20] M.E. Burulay, M.S. Mert, N. Javani, Thermodynamic analysis of a parabolic trough solar power plant integrated with a biomass-based hydrogen production system, Int. J. Hydrogen Energy 47 (2022) 19481–19501.
[21] A.M.M.I. Qureshy, I. Dincer, A new integrated renewable energy system for clean electricity and hydrogen fuel production, Int. J. Hydrogen Energy 45 (2020) 20944–20955.
[22] S. Khanmohammadi, M. Saadat-Targhi, Performance enhancement of an integrated system with solar flat plate collector for hydrogen production using waste heat recovery, Energy 171 (2019) 1066–1076.
[23] F. Yilmaz, M. Ozturk, R. Selbas, Energy and exergy performance assessment of a novel solar-based integrated system with hydrogen production, Int. J. Hydrogen Energy 44 (2019) 18732–18743.
[24] S. Sadeghi, S. Ghandehariun, Thermodynamic analysis and optimization of an integrated solar thermochemical hydrogen production system, Int. J. Hydrogen Energy 45 (2020) 28426–28436.
[25] A. Atiz, H. Karakilcik, M. Erden, M. Karakilcik, Assessment of power and hydrogen production performance of an integrated system based on middle-grade geothermal source and solar energy, Int. J. Hydrogen Energy 46 (2021) 272–288.
[26] A.M.M.I. Qureshy, I. Dincer, Energy and exergy analyses of an integrated renewable energy system for hydrogen production, Energy 204 (2020), 117945.
[27] M.D. Islam, I. Kubo, M. Ohadi, A.A. Alili, Measurement of solar energy radiation in Abu Dhabi, UAE, Appl. Energy 86 (2009) 511–515.
[28] A. B. Zavoico, "Solar Power tower design basis document, revision 0 TOPICAL," United States 2001.

[29] J.A. Duffie, W. Beckman, Solar Engineering of Thermal Processes, John Wiley & Sons, Inc, 2006.
[30] C. Xu, Z. Wang, X. Li, F. Sun, Energy and exergy analysis of solar power tower plants, Appl. Ther. Eng. 31 (2011) 3904–3913.
[31] M.S. Shahin, M.F. Orhan, F. Uygul, Thermodynamic analysis of parabolic trough and heliostat field solar collectors integrated with a Rankine cycle for cogeneration of electricity and heat, Solar Energy 136 (2016) 183–196, https://doi.org/10.1016/j.solener.2016.06.057, 2016/10/15/.